Annals of R.S.C.B., ISSN:1583-6258, Vol. 25, Issue 3, 2021, Pages. 6938 – 6949
Received 16 February 2021; Accepted 08 March 2021.

In Silico Molecular Docking Studies of Synthesized Zinc Oxide Nanoparticles using Caspace-3 Complexed with Isatin Sulfonamide as Anti-Cancer Agents

Ambika Behera[1,*], Sreenivas Enaganti[2], Shruti Awasthi[3]

[1,3](Department of Life Science, Garden City University, Bangalore, India)
[2](Department of Bioinformatics, Averinbiotech, Nallakunta, Hyderabad,India)

ABSTRACT

This study synthesized the novelZinc oxide nanoparticles (ZnO NPs) from the medicinal plant Lagerstroemia indica and for the first time performed the molecular docking of synthesized ZnO-NPs with Caspace-3 to predict the anticancer potential of the synthesized nanoparticles. An absorption peak of 302 nm obtained in the Ultraviolet-Visible (UV-Vis) spectroscopy confirmed the formation of ZnO. The X-Ray Diffraction (XRD) analysis confirmed the formation of hexagonal wurtzite structure with high crystallinity having particle size of 19.66 nm. The Scanning Electron Microscope (SEM) with Energy Dispersive Spectroscopy (EDS) micrograph confirms the purity of ZnO compound. The weight percentage and atomicity of Zn and O were found to be 77.06, 45.11 and 22.94, 54.89 respectively which matched to bulk ZnO weight percentage (80 for Zn and 20 for O). The Fourier Transform Infrared (FTIR) spectroscopy obtained strong absorption bands in the range of 459-488 cm^{-1} corresponding to Zn-O bond stretching. In silico molecular docking simulations on the crystal structure of Caspace-3 was performed to analyze the anti-cancer activity of ZnO-NPs and to determine the physiochemical and binding affinities of the synthesized ZnO-NPs against Caspace-3 (apopain or cpp32) in complex with an isatinsulfonamide inhibitor (pdb id: 1gfw) using LibDock module which may improve the quality of drug design in future work In-Vivo.

Keywords: Characterisation,In-Silico Docking study, Zinc oxide, Caspace-3

1. Introduction

Cancer, being a hereditary disease, usually remedied by traditional therapies [1,2], mostly ended up giving rise to compromised immune system [3-6]. Nanotechnology offers an opportunity to improve the therapeutic efficacies [7-9], lowering the risk of damaging the neighbouring healthy tissues and increasing the survival rate among the cancer patients [10]. Nanotechnology introduced the self-assembled nanoparticles, ranging from 1-100 nm, capable of easily capsulated, entrapped or attached to any matrix [11]. These nanomaterials are target-specific, prevent premature degradation of drug and act as image contrasting agent [12]. Zinc oxide (ZnO) due to its small size and large band width, gained much interest in the applications like anti-bacterial, anti-cancer, anti-diabetic and anti-oxidant properties [13,14].

The use of bioinformatics for the exploration of pharmacological properties of drug may be a possible therapeutic approach. Molecular docking has been widely used now-a-days [15,16]. It is a virtual simulation technique, having an energetic interaction between the Ligand and a protein. It is an emerging tool in which an interaction between the drug (Ligand) and a protein (enzyme) is used as a model to predict the preferred binding sites of protein and to analyses the orientation of the docked ligand on the active site of the protein

Annals of R.S.C.B., ISSN:1583-6258, Vol. 25, Issue 3, 2021, Pages. 6938 – 6949
Received 16 February 2021; Accepted 08 March 2021.

[17].Docking is a method which helps in predicting the favourable orientation of a small molecule bound to a target, forming a stable complex [18]. The process works with the use of docking algorithms that pose small molecules within the active site of the target destined to give a score which are designed to predict the biological activity through the assessment of interactions of binding energy between compounds and potential targets [19-23].

In cancer treatment, apoptosis is a well-recognized cell death mechanism through which cytotoxic agents kill tumor cells. In this study Caspase-3 has been considered to play an essential role in the apoptosis. Caspases are the proteases and their role in apoptosis mechanism has been studied extensively. The natural substrate of Caspases includes proteins that are actively participating in repair and cell maintenance mechanism [24-26]. The availability of inhibitors of Caspases would let assessed the potential of apoptosis of an effector Caspases [27-30].In this study theZnO-NPs has been synthesized from L. indicaand the synthesized nanoparticles has been characterized by UV-Vis spectroscopy, XRD analysis and SEM with EDS. Caspase-3 (pdb id: 1gfw) complexed with an inhibitor isatin sulfonamide has been used and its apoptotic potential has been studied against the synthesized ZnO-NPs as ligand through molecular docking studies.

2. Materials and Methods

2.1. Materials

The leaves of L. indica were collected from DRDO Township, CV Raman Nagar, Bangalore, India and were identified by Dr YasribQurishi, Associate Professor, Dept. of Biochemistry, School of Sciences, Garden City University (GCU), Bangalore, India and were also identified by the Herbarium of Botany Department, GCU, Bangalore. For the synthesis of Zinc oxide nanoparticles, Zinc acetate dehydrate (Zn $(CH_3COO)_2.2H_2O$), Sodium hydroxide (NaOH), ethanol, and deionized water (DW) were purchased from M/s Merck, India. For docking study, the human CASPASE-3 protein structure with an Isatin Sulfonamide inhibitor is retrieved from the PDB database (PDB ID: 1GFW). All the bioinformatics information were analyzed usingLibDock software, Accelrys Discovery Studio 2.1.

2.2. Preparation of Plant Extract

The leaves of L. indica were collected, washed thoroughly with DW, and then left for drying under the sun for two weeks. The dried leaves were then ground to a thin powdered extract. 3 g of powdered leaf extract was added to 125 ml of DW in a beaker. Then, it was thoroughly mixed and boiled at 70°C for 8 minutes. The solution was allowed to cool down at room temperature and filtered using Whatman filter paper. The filtrate was then collected in a flask and kept for further use.

2.3. Synthesis of Zinc Oxide Nanoparticles

In a 100 ml beaker, 0.219 g of 1 mM Zinc acetate dehydrate, $Zn(CH_3COO)_2.2H_2O$ was taken with 50 ml DW. The solution was kept in a magnetic stirrer for 1 hour. Then, 20 ml of NaOH was slowly added to the zinc acetate solution and a white precipitate was observed at the bottom. To this, 25 ml of aqueous leaf extract was added. A yellow coloration was noted after an incubation period of 1 hour. The solution was then kept in the magnetic stirrer for 3

Annals of R.S.C.B., ISSN:1583-6258, Vol. 25, Issue 3, 2021, Pages. 6938 – 6949
Received 16 February 2021; Accepted 08 March 2021.

hours. A pale-yellow color precipitate appeared which confirmed the synthesis of ZnOnanoparticles. The precipitate was separated from the reaction mixture by centrifugation at 8000 rpm for 15 minutes at 60°C. The pellets were collected and kept for drying in a hot air oven at 180°C for 2 hours and preserved in an air-tight container for further studies.

2.4. Characterization of Zinc Oxide Nanoparticles

The synthesized ZnO-NPs were characterized by UV-Vis spectrophotometer (a Perkin Elmer Lambda-2) between the wavelengths ranging from 200–800 nm by the UV visible absorption of the prepared solution sample. The XRD analysis was used to determine the structure and particle size of the powdered sample using CuKα radiation (λ = 1.542 Å; 40 kV, 30 mA) at ambient temperature. The structural morphology and shape and size of the particles was analyzed from SEM using a voltage of 15 kV. The elemental analysis of zinc and oxygen was obtained from EDS and confirmed the purity of the compound ZnO.

2.5. In-Silico Molecular Docking of Zinc oxide Nanoparticles

The molecular docking is an emerging tool in which an interaction between the drug (Ligand) and a protein (enzyme) is used as a model to predict the preferred binding sites of protein and to analyse the orientation of the docked ligand on the active site of the protein and to study the various physiological affinities of the docked ligand. In this the crystal structure of the preferred protein Caspace-3 has been retrieved from the Protein Data Bank (PDB), then the three-dimensional structure of the retrieved protein and the active site pocket residues were constructred by using the LibDock module in Accelrys Discovery Studio. Through CHARMM simulation module, LibDock, the interaction between the ligand and protein was achieved and the highest interaction energy score between the Ligand-Protein interaction was considered to be the best possible interaction andby studying its physiological affinities, a better therapeutic approach may be achievable.

3. Results and Discussion

3.1. Characterization of ZnO-NPs

The optical properties of the synthesized ZnO-NPs wereanalyzed by the UV-Vis spectrophotometer ranging from 200–800 nm. A maximum absorbance of 302 nm confirmed the formation of ZnO-NPs and is evidenced in Fig.1.

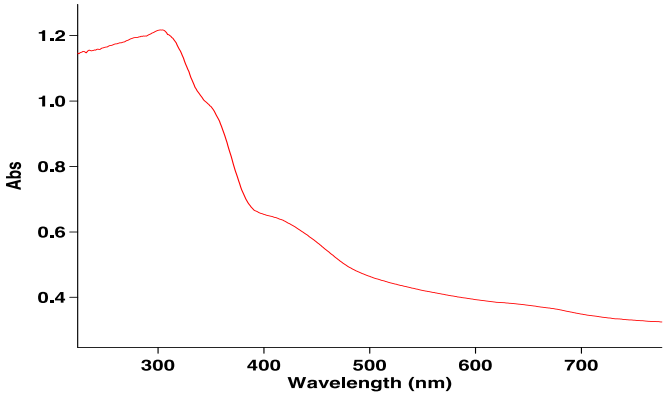

Fig.1. UV-Vis spectroscopy of ZnO-NPs.

The band gap energy (E_g) was obtained from the energy equation of Quantum Mechanics: Energy (E_g) = Planks Constant (h) × Speed of Light (C) / Wavelength

Annals of R.S.C.B., ISSN:1583-6258, Vol. 25, Issue 3, 2021, Pages. 6938 – 6949
Received 16 February 2021; Accepted 08 March 2021.

$$E_g = hc/\lambda \quad (1)$$

where, Energy (E_g) = Band gap, Planks constant (h) = 6.626×10^{-34} Joules sec, Speed of light (c) = 2.99×10^{8} meter/sec, Wavelength (λ) = Absorption peak value, which is 302 nm and 1 eV = 1.6×10^{-19} Joules. The band gap calculated was 4.11 eV. It is evidenced that zinc ions are efficiently reduced by the aqueous extract of L.indica.

FromX-Ray Diffractometry (XRD) analysis, the obtained diffraction peaks of ZnO-NPs matched with the standard JCPDS card No. 89-1397 as shown in Fig. 2.These diffraction peaks indicated the synthesized ZnO-NPs have high purity of wurtzite structure. The data also confirmed that the major purity of ZnO is 95.6% and the minor presence of $Zn(OH)_2$ is 4.4%.

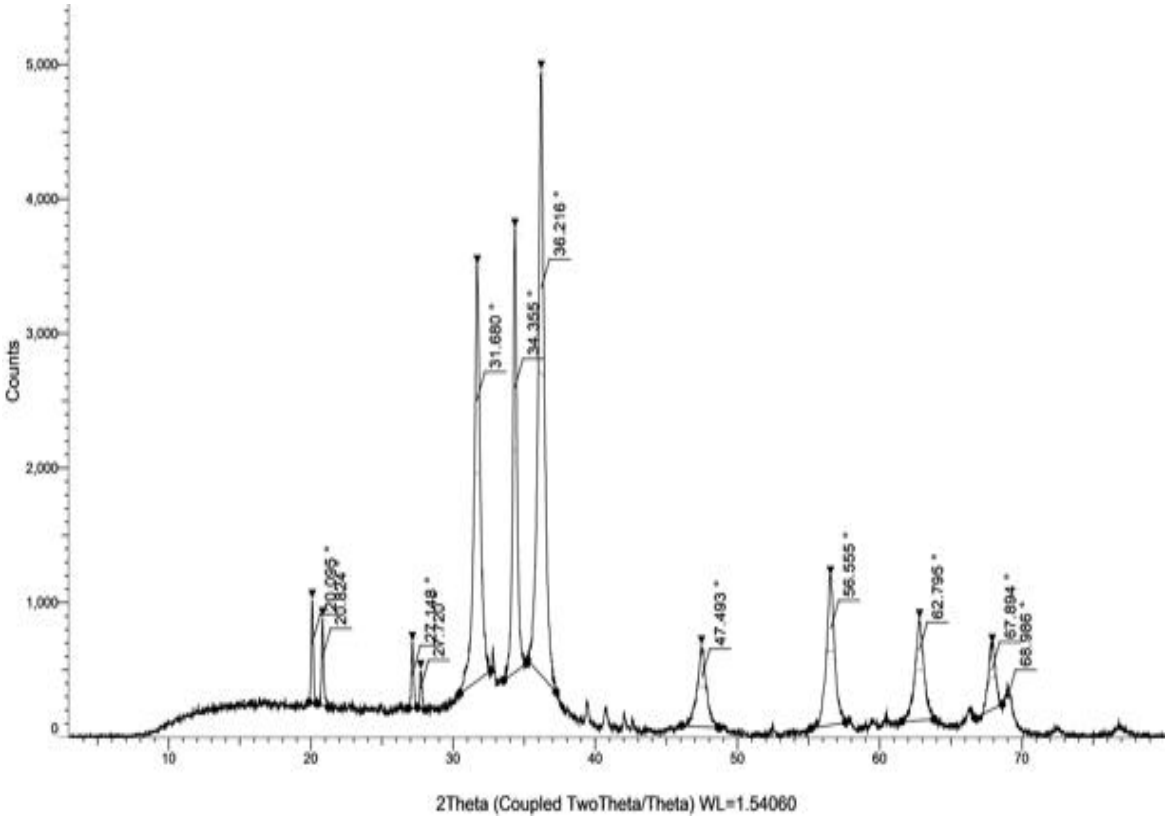

Fig.2. XRD analysis of ZnO-NPs

The diffraction peaks obtained from graph at 2θ of 31.680°, 34.355°, 36.216°, 47.493°, 56.555°, 62.795°, 67.894°, and 68.986° can be indexed with (1 0 0), (0 0 2), (1 0 1), (1 0 2), (1 1 0), (1 0 3), (2 0 0), and (1 1 2) planes. The average crystallite size (D) was calculated using Debye–Scherrer's formula:

$$\text{Crystallite Size } (D) = \frac{0.89\lambda}{d\cos\theta} \quad (2)$$

where, 0.89 is the Scherrer's constant, λ is the wavelength of X-rays (0.154), θ is the Bragg's diffraction angle, and d is the Full Width at Half Maximum (FWHM) of diffraction peak. The average crystallite size was found to be 19.66 nm.

SEM images of the synthesized ZnO-NPs showed that most of the particles were hexagonal. Some of these images in 5 nm scale indicate a few amorphous structures as confirmed by XRD data as shown in Fig. 3 (a) and the EDS micrograph in Fig.3 (b) shows the purity of the ZnO compound. The weight percentage and atomicity of Zn and O were

Annals of R.S.C.B., ISSN:1583-6258, Vol. 25, Issue 3, 2021, Pages. 6938 – 6949
Received 16 February 2021; Accepted 08 March 2021.

found to be 77.06, 45.11 and 22.94, 54.89, respectively, that matched with the bulk ZnO weight percentage (80 for Zn and 20 for O).

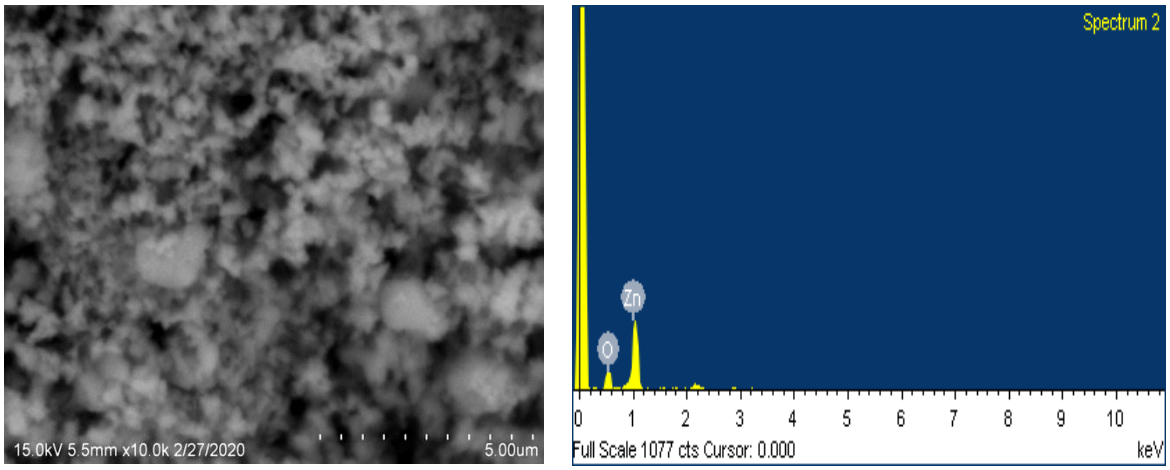

(a) (b)

Fig.3. (a) SEM image of ZnO-NPs and (b) EDS micrograph of ZnO-NPs

3.2. In-Silico Molecular Docking

To study the behavioural properties and the binding affinities of the synthesized ZnO-NPs with Caspase-3 (apopain or cpp32) in complex with an isatinsulfonamide inhibitor (pdb id: 1gfw) using LibDock module in Accelrys Discovery Studio 2.1.LibDock is a high-throughput site-featured docking algorithm [31]. Figure4represented the crystal structure of Caspase-3 (pdb id:1gfw). The information on the retrieved protein crystal structure from the PDB database is presented in Table1.

Table.1. Physiochemical Properties of Caspase-3 retrieved from PDB database

Physiochemical Properties of Protein (Caspace-3)	
Parameters	Value
Cell Space Group	23
Crystallographic Resolution	2.8 A °
Molecular Weight	27,375.2
Amino-acid Chain Name	AB
Number of Amino-acid Residues	238

Annals of R.S.C.B., ISSN:1583-6258, Vol. 25, Issue 3, 2021, Pages. 6938 – 6949
Received 16 February 2021; Accepted 08 March 2021.

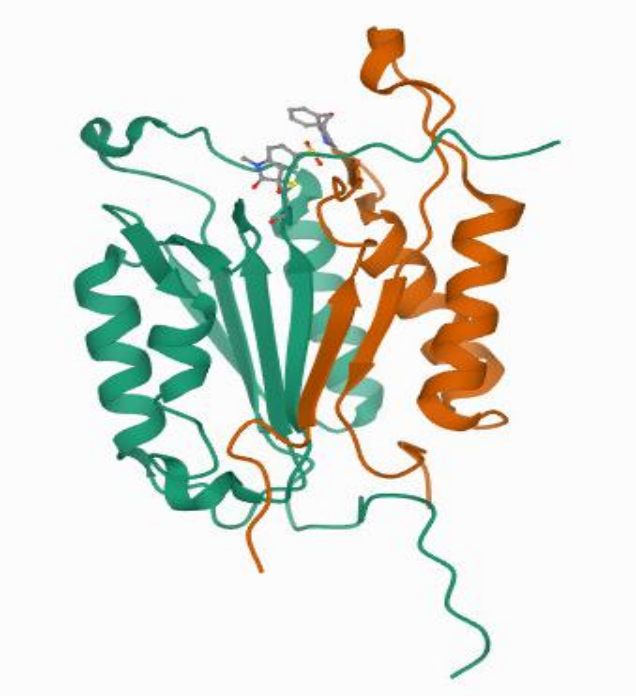

Fig.4. Crystal structure of Caspase-3 (apopain or cpp32) in complex with an isatin sulfonamide inhibitor (pdb id: 1gfw)

3.2.1. Three-Dimensional (3D) Structure of Caspase-3

The 3D structure of the protein Caspase-3 from Homosapiens,expressed in E. coli, was determined by using the homology modelling methods of Discovery Studio (DS). Homology modelling was for the alignment of the target sequence and the sequences of known structures of one or more proteins as templates, which resembled the structure of the query sequence. The sequence alignment and template structure are then used to generate a structural model of the target[32]. Table2 represents the secondary structure of Caspase-3 analysed by LibDock module. The 3D structure of the protein was retrieved and presented in Fig.5.

Table.2. Secondary Structure of Caspase-3 predicted and analysed by LibDock module in Accelrys DiscoverStudio 2.1.

Sequence

Chain A

SGISLDNSYK MDYPEMGLCI IINNKNFHKS TGMTSRSGTD VDAANLRETF
RNLKYEVRNK NDLTREEIVE LMRDVSKEDH SKRSSFVCVL LSHGEEGIIF
GTNGPVDLKK ITNFFRGDRC RSLTGKPKLF IIQACRGTEL DCGIE

Chain B

HKIPVDADFL YAYSTAPGYY SWRNSKDGSW FIQSLCAMLK QYADKLEFMH
ILTRVNRKVA TEFESFSFDA TFHAKKQIPC IVSMLTKELY FYH

Comparison of actual sequence versus PDB SEQRES records

End of chain A appears to be missing - residues: THR ASP
Start of chain B appears to be missing - residues: ASP MET ALA CYS

Incomplete or Invalid Residues

A:GLU173

Active Sites

Active Site AC1: MET61 ARG207 LYS57 SER205 SER58 PHE256 TRP206 GLY122 TYR204 HIS121 CYS163

Annals of R.S.C.B., ISSN:1583-6258, Vol. 25, Issue 3, 2021, Pages. 6938 – 6949
Received 16 February 2021; Accepted 08 March 2021.

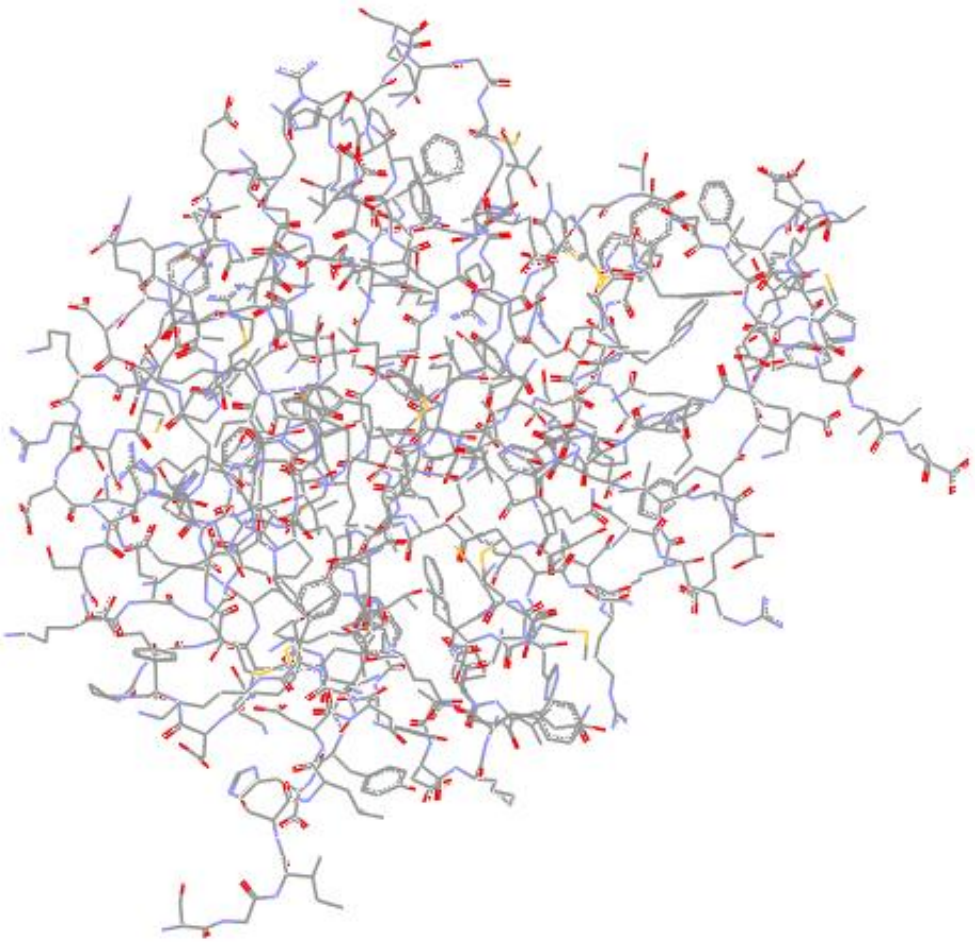

Fig.5. Three-dimensional structure of caspase-3 (apopain or cpp32) in complex with an isatin sulfonamide inhibitor, represented in wireframe.

3.2.2. Protein Preparation

The human CASPASE-3 protein structure in complex with an isatinsulfonamide inhibitor. Is retrieved from the PDB database (PDB ID: 1GFW) having a resolution of 2.8 A °and is imported into Accelrys Discovery Studio 2.1. Further using the clean protein protocol within Discovery Studio, the protein is prepared for correcting the lack of hydrogen atoms, missing atoms and residues, incorrect atom order in amino acids, to complete the protein chain. Water molecules are removed, and protonating all the residues at a ph of 7.4 conditions is done, thus allowing the protonation of arginine and lysine side chains and deprotonation of glutamate and aspartate side chains. The protonation of histidine side chains is selective in accordance with their context in the target. All the heteroatoms are removed except isatinsulfonamide inhibitor which is used later for defining the binding site. To the protein complex of Caspase-3 (apopain or cpp32) with an isatinsulfonamide inhibitor, CHARMM force field is applied for protein preparation with potential energy of -14311.70998 kcal/mol, Van der Waals energy of -1762.12583 kcal/mol and an initial RMS (Root Mean Square) gradient energy of 0.96320 kcal/mol. By using smart minimizer algorithm with a maximum number of steps 1000 and RMS gradient 0.1, energy minimization is performed that carry forward using steepest descent and conjugate gradient algorithm till the protein complex makes a grade of convergence

Annals of R.S.C.B., ISSN:1583-6258, Vol. 25, Issue 3, 2021, Pages. 6938 – 6949
Received 16 February 2021; Accepted 08 March 2021.

gradient 0.001 kcal/mol. Figure.6. represented the prepared protein structure model in wireframe [33].

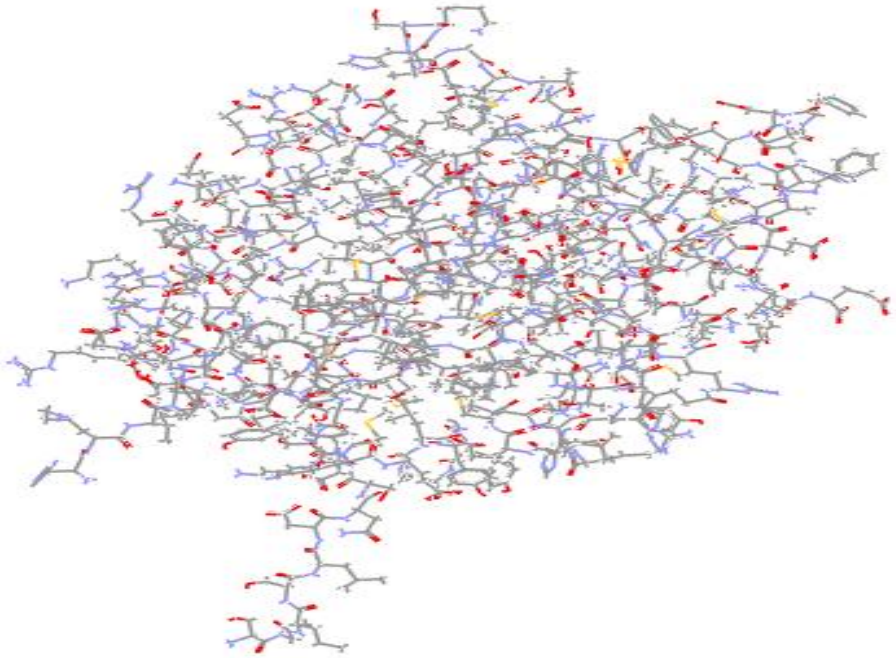

Fig.6. Prepared Protein structure represented in Wireframe

3.2.3. Identification of Active Site Pocket residues of 1gfw:

After the protein complex is energy minimized, the possible binding site of the human Caspase-3 is predicted by using the Define and Edit Binding Site tool in Accelrys Discovery Studio 2.1. The protein binding site was determined based on the occupied volume of the known ligand Isatinsulfonamidein the active site. The co-crystallized Isatinsulfonamide molecule was first selected, and a sphere was created around the molecule using define sphere from the selection optionat a radius of 10 A ° and setting the X,Y and Z-axis as 38.049600,33.550400 and 26.968400, respectively from the selection option. Figure7 represents the active pocket site residues of the prepared protein.

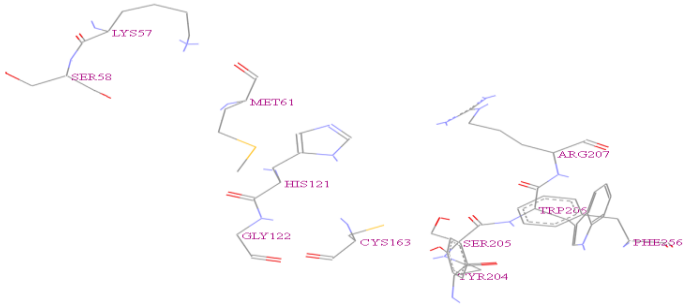

Fig.7. Active site pocket residues of 1gfw

Annals of R.S.C.B., ISSN:1583-6258, Vol. 25, Issue 3, 2021, Pages. 6938 – 6949
Received 16 February 2021; Accepted 08 March 2021.

3.2.4. Preparation of Ligand

Using ACD/ChemSketch (12.0), the two-dimensional structures of all the compound of ZnO are drawn and saved in mol file format. The saved compounds are imported into Accelrys Discovery Studio 2.5 (DS) and ligand preparation with constraint parameters such as consistency of ionization state of oxygen and nitrogen atoms at physiological pH, the addition and deletion of hydrogen is done with CHARMMForce field and converted to 3D structures using catalyst algorithm in Discovery Studio and represented in Fig. 8.

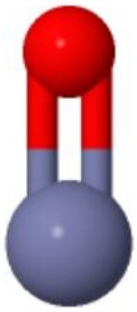

Fig.8. Preparation of Ligands

3.2.5. Molecular Docking Result

For the docking of ligands into the protein binding pockets and to determine the affinities of the docked ligand, a molecular docking studies has been carried out using LibDock.The selection of the best docked ligand was chosen on the basis of the interaction energy between the ligand and the protein according to the LibDock score and also the formation of hydrogen bond between the protein-ligand complex and the receptor docking conformation was calculated with the 'Analyze Ligand Poses' process analysis.From the Docking interaction analysis, the best confirmation of the docked complex, shown in Fig.9, achieved ahigh interaction energy of 13.234 kcal/mol and calculated binding energy of -64.74280 kcal/mol.

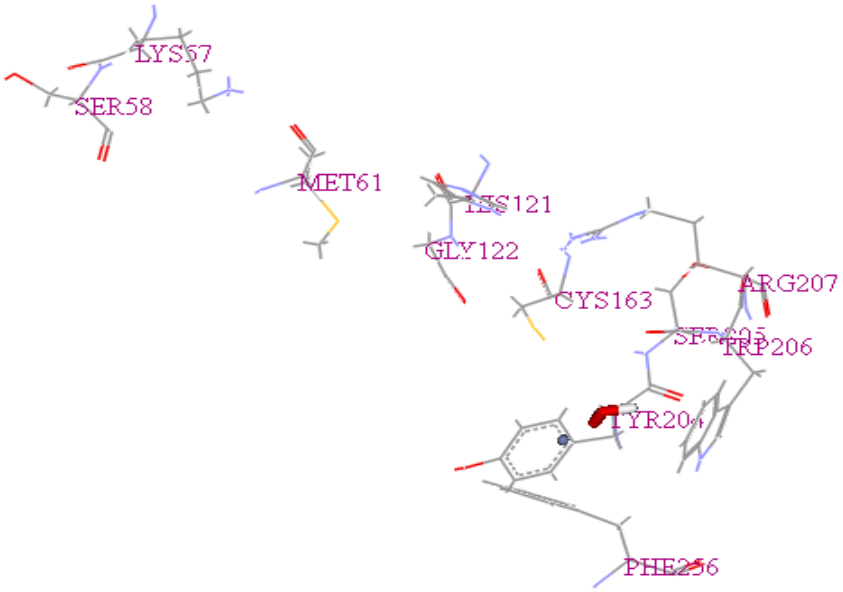

Fig.9. Receptor-Ligand interaction of ZnO with active binding sites of Caspase-3(1gfw)

4. Conclusion

In this study ZnO NPs have been successfully synthesized from Lagerstroemia indica. The synthesized nanoparticles were characterized by UV-Vis, XRD, SEM with EDS and FTIR. The optical absorption of UV-Vis spectroscopy confirmed the formation of ZnO nanoparticles. SEM and EDS data recommended the presence of crystallinity of the synthesized nanoparticles with purity of ZnO compound. XRD analysis confirmed the formation of hexagonal wurtzite structure of ZnO-NPs and through Debey Scherrer's formula, the average crystallite size was found to be 19.66 nm. Finally, the In-silico molecular docking of ZnO with binding active sites of protein, Caspase-3 has been achieved. The analysed docking result determined that the binding sites of the targeted protein with the compound ZnO-NPs has shown significant interaction with a high binding energy, suggesting an alteration in the physiochemical processes involved in the apoptosis mechanism. This wouldimprove their anti-cancer potential which may act as a potent drug in various cancer diseasesfor future perspectives.

5. Acknowledgement

The authors would like to thank M/s Sophisticated Test and Instrumentation Centre (STIC), Cochin University of Science and Technology, Cochin - 682 022, Kerala, India for analytical testing and M/s Averin Biotech Biotechnology Training Company, Hyderabad, Telangana - 500044 for cytotoxicity experiments. The authors also thank the Chancellor, Dr. Joseph V.G., Garden City University (GCU), Bangalore, India for his encouragement and support. The authors would like to thank Dr YasribQurishi for her guidance throughout the study.

References

[1] R.G. Prosnitz, M.B. Patwardhan, G.P. Samsa, et al. Quality measures for the use of adjuvant chemotherapy and radiation therapy in patients with colorectal cancer: A systematic review, Cancer, 107(10),2006, 2352-2360.
[2] M. Ferrari, Cancer nanotechnology: opportunities and challenges, Nat Rev Cancer, 5(3), 2005, 161-71.
[3] K.C. Li, S.D. Pandit, S. Guccione, et al., Molecular imaging applications in nanomedicine,Biomed Microdevices, 6(2),2004, 113-116.
[4] S.F. Hashemi, N. Tasharrofi, and M.M. Saber, Green synthesis of silver nanoparticles using Teucrium polium leaf extract and assessment of their antitumor effects against MNK45 human gastric cancer cell line,J Mol Struc, 1208,2020, 127889.
[5] R. Langer, Drug delivery and targeting,Nature, 392(6679 Suppl),1998, 5-10.
[6] P. Khandel, R.K. Yadaw, D.K. Soni, et al., Biogenesis of metal nanoparticles and their pharmacological applications: present status and application prospects,J Nanostruct Chem, 8,2018, 217–254.
[7] R. Selot, S. Marepally, P.K. Vemula, et al., Nanoparticle coated viral vectors for gene therapy. CurrBiotechnol, 5(1),2016, 44-53.
[8] M.G. Cascone, L. Lazzeri, C. Carmignani, et al.,Gelatin nanoparticles produced by a simple W/O emulsion as delivery system for methotrexate,J Mater Sci Mater Med, 13(5),2002, 523-526.

[9] D. Suresh, R.M. Shobharani, P.C. Nethravathi, et al., Artocarpus gomezianus aided green synthesis of ZnO nanoparticles: luminescence, photocatalytic and antioxidant properties, Spectrochim.Acta A Mol. Biomol. Spectrosc, 141,2015, 128–134.
[10] J. Qu, X. Yuan, X. Wang, et al., Zinc accumulation and synthesis of ZnO nanoparticles using Physalis alkekengi L,Environ. Pollut, 159(7),2011, 1783–1788.
[11] M.L. Kahn, T. Cardinal, B. Bousquet, et al., Optical properties of zinc oxide nanoparticles and nanorods synthesized using an organometallic method,ChemPhysChem, 7(11),2006, 2392-2397.
[12] O. Lupan, L. Chow, S. Shishiyanu, et al., Nanostructured zinc oxide films synthesized by successive chemical solution deposition for gas sensor applications,Materials Research Bulletin, 44(1),2009, 63–69.
[13] K. Elumalai, and S. Velmurugan, Green synthesis, characterization and antimicrobial activities of zinc oxide nanoparticles from the leaf extract of Azadirachta indica,Appl. Surf. Sci, 345,2015, 329–336.
[14] G. Sangeetha, S. Rajeshwari, and R. Venckatesh, Green synthesis of zinc oxide nanoparticles by aloe barbadensis miller leaf extract: structure and optical properties, Mater. Res. Bull, 46 (12),2011, 2560–2566.
[15] D.B. Kitchen, H. Decornez, J.R. Furr, and J. Bajorath, Docking and scoring in virtual screening for drug discovery, methods and applications, Nat Rev Drug Discov., 3, 2004, 935-949.
[16] A.R. Leach, B.K. Shoichet, and C.E. Peishoff, Prediction of proteinlig and interactions. Docking and scoring: successes and gaps,J Med Chem., 49,2006, 5851-5855
[17] S.F. Sousa, P.A. Fernandes, and M.J. Ramos, Protein-ligand docking: current status and future challenges,Proteins 65,2006, 15-26.
[18] O. Trott, and A.J. Olson, AutoDock Vina: improving the speed and accuracy of docking with a new scoring function, efficient optimization, and multithreading,J Comput Chem, 31,2010, 455-461.
[19] V. Asati, S.S. Thakur, N. Upmanyu, and S.K. Bharti, Virtual screening, molecular docking, and DFT studies of some thiazolidine-2, 4-diones as potential PIM-1 kinase inhibi- tors, ChemistrySelect, 3, 2018, 127–135.
[20] M.S. Ali, M. Altaf, and H.A. Al-Lohedan, Green synthesis of biogenic silver nanoparticles using Solanum tuberosum extract and their interaction with human serum albumin: evidence of “corona” formation through a multi-spectroscopic and molecular docking analysis, J. Photochem. Photobiol. B, 173, 2017, 108–119.
[21] M. Majumdar, S. Khan, S. Biswas, et.al., In vitro and in silico investigation of anti-biofilm activity of Citrus macroptera fruit extract mediated silver nanoparticles, Journal of Molecular Liquids, 302,2020,112586.
[22] K. Giannousi, G. Geromichalos, D. Kakolyri, et.al., Interaction of ZnO Nanostructures with Proteins: In Vitro Fibrillation/Antifibrillation Studies and in Silico Molecular Docking Simulations, ACSChemical Neuroscience, 11(3), 2020, 436-444.
[23] E.L. Gelamo, C.H.T.P. Silva, H. Imasato, and M. Tabak, Interaction of bovine (BSA) and human (HSA) serum albumins with ionic surfactants: spectroscopy and modelling. Biochim. Biophys. Acta, 1594 (1), 2002, 84−99.

[24] D. Lee, A.L. Scott, and J.L. Adams, Potent and Selective Nonpeptide Inhibitors of Caspases 3 and 7 Inhibit Apoptosis and Maintain Cell Functionality, Journal of Biological Chemistry, 275 (21), 2000, 16007–16014
[25] A.G. Porter,and R.U. Jänicke, Emerging roles of caspase-3 in apoptosis, Cell Death Differ, 6(2), 1999, 99-104.
[26] D.W. Nicholson, and N.A. Thornberry, Caspases: killer proteases, Trends Biochem Sci. 22(8), 1997, 299-306.
[27] N.A. Thornberry, T.A. Rano, and E.P. Peterson, A combinatorial approach defines specificities of members of the caspase family and granzyme B. Functional relationships established for key mediators of apoptosis, J. Biol Chem, 272(29), 1997, 17907-17911.
[28] S. Hashimoto, R.L. Ochs, S. Komiya, and M. Lotz, Linkage of chondrocyte apoptosis and cartilage degradation in human osteoarthritis, Arthritis Rheum, 41(9), 1998, 1632-1638.
[29] M.E. Nuttall, M. Gowen, and M. W. Lark, Apoptosis and inflammatory disease: osteoarthritis, In: Winkler J.D. (eds) Apoptosis and Inflammation. Progress in Inflammation Research. Birkhäuser, Basel, 1999, 163-179.
[30] A.P. Hollander, I. Pidoux, and A. Reiner, Damage to type II collagen in aging and osteoarthritis starts at the articular surface, originates around chondrocytes, and extends into the cartilage with progressive degeneration, J Clin Invest. 96(6), 1995, 2859-2869.
[31] D.J. Diller, K. Merz, and K.M. Merz Jr.,High throughput docking for library design and library prioritization, Proteins Structure Function and Bioinformatics, 43(2), 2001, 113 – 124.
[32] J. Shi, T.L. Blundell, and K. Mizuguchi, FUGUE: sequence-structure homology recognition using environment-specific substitution tables and structure-dependent gap penalties, J Mol Biol., 310(1), 2001, 243-257.
[33] R.Vadlakonda, R. Nerella, and S.Enaganti, Theoretical Studies on Azaindoles as Human Aurora B Kinase Inhibitors: Docking, Pharmacophore and ADMET Studies, Interdiscip Sci Comput Life Sci, 10(3), 2018, 486-499.